HHS Public Access

Author manuscript

Nat Chem. Author manuscript; available in PMC 2023 February 01.

Published in final edited form as:

Nat Chem. 2022 February ; 14(2): 216–223. doi:10.1038/s41557-021-00835-7.

Arene Radiofluorination Enabled by Photoredox-Mediated Halide Interconversion

Wei Chen[1], **Hui Wang**[1], **Nicholas E. S. Tay**[2,#], **Vincent A. Pistritto**[2], **Kang-Po Li**[1], **Tao Zhang**[1], **Zhanhong Wu**[1], **David A. Nicewicz**[2,*], **Zibo Li**[1,*]

[1]Biomedical Research Imaging Center, Department of Radiology, and UNC Lineberger Comprehensive Cancer Center, University of North Carolina- Chapel Hill, Chapel Hill, NC 27514, USA.

[2]Department of Chemistry, University of North Carolina at Chapel Hill, Chapel Hill, North Carolina, 27599-3290, United States

Abstract

Positron emission tomography (PET) is a powerful imaging technology that could visualize and measure metabolic processes *in vivo* and/or obtain unique information about drug candidates at early stages. Identification of new and improved molecular probes plays a critical role in PET, but its progress is limited in many situations due to the lack of efficient and simple labeling methods to modify biologically active small molecules and/or drugs. Although various approaches have been reported, current methods to radiofluorinate unactivated arenes are still relatively limited, especially in a simple and site-selective way. Here we disclose a method for constructing C–^{18}F bonds through direct halide/^{18}F conversion in electron-rich halo(hetero)arenes. [^{18}F]F^{-} is efficiently introduced into a broad spectrum of readily available aryl halide precursors in a site-selective manner under mild photoredox conditions. Notably, we demonstrate that our direct ^{19}F/^{18}F exchange method enables rapid PET probe diversification through the preparation and evaluation of a [^{18}F]-labeled *O*-methyl tyrosine library, leading to the discovery of new cancer imaging agents. This strategy also results in the high-yielding synthesis of the widely used PET agent *L*-[^{18}F]FDOPA from a readily available *L*-FDOPA analog. Taken together, our photoredox-mediated halide/^{18}F interconversion strategy offers a new chemical tool for preparing new and clinically significant ^{18}F-labeled PET agents.

[*]Corresponding Author: nicewicz@unc.edu (D.A.N.), ziboli@med.unc.edu (Z. L.).

[#]**Present Addresses:** N.E.S.T.: Department of Chemistry, Columbia University, New York, New York 10027, United States

Author contributions

W.C. discovered the halides/^{18}F conversion project, prepared the substrates, ^{19}F-standards and performed the radiolabeling reactions. H.W. conducted the animal imaging studies and performed PET imaging data collection and analysis. N.E.S.T. was involved in the discovery of the ^{19}F/^{18}F exchange reaction. V.A.P. and K.L. assisted in the synthesis and analysis of substrates. T.Z. assisted in the animal studies. Z.W. contributed to the initial discussion. D.A.N. and Z.L. conceived and supervised the project and experiments. W.C., D.A.N. and Z.L. wrote the manuscript. N.E.S.T. and V.A.P assisting in editing the manuscript.

Competing interests

The authors have filed a provisional US patent on the basis of the research in this manuscript.

Introduction

Positron emission tomography (PET) is a routinely-used non-invasive imaging technique for the real-time diagnosis and monitoring of human diseases, most notably being oncological and neurological disorders[1,2]. Advances in radiotracer development have accelerated the clinical adoption of PET and fostered a growing interest in robust methodologies for synthesizing PET agents via the late-stage installation of short-lived radionuclides[3]. Because many small molecule pharmaceuticals and therapeutics contain aromatic or heteroaromatic systems within their framework[4–7], it is highly desirable to introduce radionuclides on these moieties in a synthetically facile and efficient manner. Late stage radiolabeling is especially preferred considering the decay of short lived PET isotopes[8–11]. Fluorine-18 (^{18}F) is arguably the most widely used short-lived PET isotope ($t_{1/2}$ ~110 min) due to its excellent imaging properties, wide availability and ideal half-life. A common strategy used for constructing aryl C(sp^2)–^{18}F bonds is nucleophilic aromatic substitution (S_NAr), which substitutes a (pseudo)halide with ^{18}F fluoride ($^{18}F^-$) (Fig.1A). This strategy is routinely used for the synthesis of PET agents with high molar activity[12–15] but is limited to electron-deficient (hetero)aromatic systems[16]. Consequently, systems for the nucleophilic radiofluorination of electron-neutral and -rich aromatics have been investigated over the past decade[3,17]. Progress towards this goal have focused on either transition-metal mediated methods[18,19,20–24] or the development of specialized nucleofuges[25–29], with several of the aforementioned strategies adapted for automation[18,20–25,28,30,31], which streamlines their translation to clinical use. As a major substrate class for arene functionalization, aryl (pseudo)halides are commonly used intermediates on route to synthesizing organometallic or prefunctionalized arene precursors for radiofluorination (such as aryl-palladium[18]/nickel complexes[19], aryl boronic acids[22]/esters[20], aryl stannanes[23] and aryl iodonium salts/ylides[21,24,25]) (Fig.1B). Clearly, methods that could directly radiofluorinate electron-rich aryl halides are highly desired due to its simplicity. However, there are scarce radiofluorination examples for unactivated aryl (pseudo)halides except a recent method disclosed by the Scott and Sanford groups which allowed the ligand-directed conversion of aryl halides to radiofluorinated arenes using an NHC-copper complex[31]. While the installation of ^{18}F in electron-neutral and -rich arenes is impressive, the requisite substrate directing group could limit the generality of this approach (Fig.1C). Additionally, this method is limited to aryl iodides and bromides, with chloro-arenes being minimally reactive and no ^{19}F/^{18}F exchange product observed. Given the dearth of methods for the direct radiofluorination of electron-rich aryl chlorides and fluorides, developing a simple strategy to directly radiofluorinate these motifs is highly desired, especially considering their stability and abundance in therapeutics[7,32,33]. Importantly, the success of this approach would also enable the direct conversion of readily available fluorinated therapeutics into ^{18}F-labeled radiopharmaceuticals through simple late-stage ^{19}F/^{18}F exchange[34–36].

We recently disclosed two acridinium photoredox-mediated methods for arene radiofluorination in which the photoactivated acridinium oxidizes arenes to arene cation radicals, thus enabling site-selective radiofluorination of C(sp^2)–H[37] and C(sp^2)–O[29] bonds. Inspired by our previous success, we explored the feasibility of directly converting an aryl halide into their ^{18}F-labeled congeners for electron-rich arenes. Upon single

electron oxidation, we envisioned the resulting electron-deficient cation radical would capture the $^{18}F^-$ at the halide-bearing carbon. Subsequent reduction and expulsion of the halide nucleofuge would furnish the desired radiofluorinated arene (Fig. 1C). This radiofluorination strategy would obviate the need for lengthy, multi-step precursor synthesis, greatly simplifying product isolation, and open up new ways to prepare clinically significant PET agents.

Results

To evaluate whether acridinium photocatalysts could promote halide/^{18}F exchange in electron-rich arenes, we adapted our previously-reported radiodeoxyfluorination conditions to 1-chloro-4-methoxybenzene (1-Cl) with the intent of promoting halide extrusion. Irradiating a reaction solution containing the substrate, [^{18}F]*n*-tetrabutylammonium fluoride ([^{18}F]TBAF) and acridinium S1 in a multicomponent DCE/*t*-BuOH/MeCN solvent system with a 450 nm laser under consistent air bubbling for 30 min leads to the formation of **1-^{18}F**, albeit in 1.7% radiochemical conversion (RCC) as calculated by HPLC isolation. In our previous (radio)deoxyfluorination study[29], we found that methoxy groups were ineffective due to the competitive deprotonation of acidic *O*-methyl C–H bonds upon formation of the arene cation radical — this deleterious pathway competes with extrusion of halide under aerobic conditions[38]. To circumvent this potential side-reaction, the radiofluorination of 1-Cl was conducted under a nitrogen atmosphere, which successfully increased the isolation yield of **1-^{18}F** to 12.8 ± 0.3% (n=3) with 71.25 GBq/μmol molar activity (A_m).

With these preliminary results, we then screened other nucleofuges commonly used in S_NAr reactions (Fig 2). The radiofluorination of haloarene 1-bromo-4-methoxybenzene (**1-Br**) yields a comparable RCC with **1-Cl** whereas 1-iodo-4-methoxybenzene (**1-I**) was surprisingly less reactive, with a ten-fold lower RCC observed. Interestingly, 1-fluoro-4-methoxybenzene (**1-F**) was found to provide the highest yield of radiofluorinated product through direct ^{19}F/^{18}F exchange (79.7%). This observation represents a significant breakthrough in the field because it allows simple and efficient conversion of electron-rich fluorinated bioactive compounds or pharmaceuticals to ^{18}F-labelled PET radiotracers directly. Prior reports of fluoroarene ^{19}F/^{18}F exchange have been restricted to electron-deficient compounds and generally require relatively high temperatures[36,39]. A potential limitation of this strategy is the decreased molar activity (A_m) by virtue of using the HPLC-inseparable ^{19}F-fluoroarene. However, A_m values can be significantly improved by limiting the amount of aryl fluoride, which has been demonstrated previously[36a,40]. Next, we found that aryl triflate **1-OTf** was successfully radiofluorinated, albeit with lower yields. Interestingly, 1-methoxy-4-nitrobenzene (**1-NO_2**) was unreactive despite the well-documented substitution of nitro nucleofuges in traditional S_NAr.

To better understand the effect of substitution pattern on the halogen/^{18}F interconversion, we evaluated a range of aromatic and heteroaromatic substrates (Fig 2). Increasing alkylation at the α-carbon relative to oxygen in *O*-alkylated 4-chlorophenol derivatives resulted in a 2- to 4-fold RCC increase, suggesting that labile C–H bonds adjacent to the *O*-atom be inhibitory to the reaction (**2**, **3**, **4-Cl**, **5-Cl**). This effect is less pronounced for ^{19}F to ^{18}F conversion, where minimal RCC differences were observed. For example, both **4-F** and

5-F were obtained in excellent RCC based on HPLC isolation. We also performed the halide/^{18}F interconversion reactions with blue LED instead of laser on substrates **5-Cl** and **5-F**. We were pleased to find that the Cl/^{18}F conversion proceeded on **5-Cl** albeit with lower RCC. Meanwhile, the ^{19}F/^{18}F isotopic exchange on **5-F** afforded comparable RCC with LED irradiation. A *meta*-methyl substituent (**6**) resulted in moderate RCC improvement, while substituents *ortho* to the chlorine nucleofuge resulted in more efficient halide/^{18}F conversion (**7–9**). This observation is tentatively attributed to the enhanced stability of a putative captodative cation radical intermediate invoked in our previous findings[29,41]. 2,4-Dimethoxy-substituted aryl halides (**10-Cl**, **10-Br**, **10-I**) were labelled with $^{18}F^{-}$ leading to **10-^{18}F** in good, moderate and low RCCs respectively. Interestingly, **10-NO$_2$** which is more electron rich than mono-methoxy **1-NO$_2$**, was successfully radiofluorinated with 48.3% RCC. This observation suggests that the lack of reactivity with **1-NO$_2$** is likely due to a mismatch in redox potentials between **1-NO$_2$** and the acridinium catalyst. The radiofluorination of 2,4,6- and 2,3,4-substituted chlorobenzenes (**11–14**) was accomplished with moderate to excellent RCCs. Desymmetrization of dihalogenated aromatics (**15** and **16**) was also demonstrated, although the reduced solubility of dibrominated **16** resulted in a lower RCC than the more soluble dichlorinated analog (**15**). More pronounced changes in radiofluorination efficiency were observed *O*-alkylated haloarenes bearing *ortho*-nucleofuges (**17–20**). Chloro- and fluoro-naphthalenes and their alkoxy-substituted derivatives were also successfully radiofluorinated (**21-23**). Aryl fluorides containing protected amines (**24, 25-F, 26–27**) undergo ^{19}F/^{18}F conversion with moderate to good RCC under the standard labelling conditions, with aryl chloride **25-Cl** demonstrating lower radiofluorination efficiency. Chloro- and fluoro-substituted heterocycles were also successfully radiofluorinated via Cl/^{18}F or ^{19}F/^{18}F conversion, as demonstrated for carbazoles **28-F** and **28-Cl**, *N*-benzyl indolinone **29**, 3,3-dimethy-3*H*-indoles **30-F** and **30-Cl**, *N*-methyl indazoles **31** and **32**, benzo[*b*]thiophene **33**, quinazoline-2,4(1H,3H)-dione **34**, pyridine **35**, and chromanone **36**. Additionally, 4-(arylamino)quinazoline fragment **37** and its analog **38**, common pharmacophores in kinase inhibitors[42], were found to be competent substrates for direct ^{19}F/^{18}F exchange. Several substrate limitations exist for this methodology (Supplementary Figure 138). Generally, the presence of an activated benzylic group or α-heteroatom methylene unit leads to decreased yield or results in no reaction, likely because the deprotonation by fluoride is kinetically favored. Additionally, substates bearing more oxidizable functional groups other than the halogenated aromatic ring under light irradiation, for example, unprotected amines or alcohols would lead to competing electron transfer pathways and thus inhibit the halogen-^{18}F exchange process. Lastly, substrates where the halogen and methoxy are *meta* to each other, tend to give low or no yield under current conditions.

To probe the chemo- and regioselectivity of the halide/^{18}F conversion, we studied substrates bearing more than one potential halogen nucleofuge (Fig. 3a). Radiofluorination of compound **39** provides both Br/^{18}F and Cl/^{18}F conversion products (**15-^{18}F**, **16-^{18}F**) in 1:1.4 ratio in slight favor of chlorine substitution. When the bromide was shifted to the *meta* position relative to the methoxy groups (**40**), selective Cl/^{18}F conversion (**40-^{18}F**) was observed. These results suggest that 1) chlorine is a better nucleofuge than bromine, and 2) the site of S_NAr is largely dependent on arene electronics. Next, we explored the

selectivity between Cl/^{18}F conversion (S_NAr) and bimolecular nucleophilic substitution (S_N2), which is a commonly employed strategy to introduce ^{18}F into alkyl groups in PET radiotracer design[3]. Compound **41** is a substrate containing both aryl and alkyl chlorides (Fig. 3b). Selective Cl/^{18}F conversion (S_NAr) (**41-^{18}F**) is observed under photoredox conditions while heating the reaction to 100 °C results in exclusive [^{18}F]F^- displacement of the alkyl chloride (**41-^{18}F-a**). Next, we probed the chemoselectivity between electron-rich and electron-deficient arenes within one molecule (Fig. 3c). Using compound **42** as our model substrate, we obtained exclusive ^{19}F/^{18}F conversion (**42-^{18}F**) with no traditional S_NAr product (**42-^{18}F-a**)[43]. Taken together, these results suggest that our halide exchange strategy is selective for electron-rich substrates using photoredox conditions without $^{18}F^-$ substitution of alkyl halides and electron-deficient aryl halides.

We next applied our halide/^{18}F interconversion strategy towards the radiolabeling of known pharmaceuticals and bioactive molecules (Fig. 4a). Clofibrate (**43**) and Boc-protected atomoxetine (**44**) were directly converted to ^{18}F-fluorinated analogs (**43-^{18}F**, **44-^{18}F**) through aryl-Cl/^{18}F exchange while ^{18}F-labelled flurbiprofen methyl ester (**45**) and diflunisal (**46**) were obtained (**45-^{18}F, 46-^{18}F**) through direct ^{19}F/^{18}F conversion. Mono-Boc protected fluorodopamine (**47-F**) was efficiently labelled through ^{19}F/^{18}F conversion (**47-^{18}F**) in excellent RCC. Fluorinated dopamine **47-^{18}F** could also be synthesized through Cl/^{18}F exchange with a lower RCC but higher molar activity. ^{18}F-labelled 2-phenoxyaniline derivatives have been investigated as translocator protein (TSPO)-specific PET agents for neuroinflammation imaging[44]. Using our aryl-Cl/^{18}F conversion method, ^{18}F successfully replaced the chlorides in 2-phenoxyaniline derivatives, leading to potential new imaging agents (**48-^{18}F**, **49-^{18}F**, and **50-^{18}F**) targeting TSPO. Additionally, [^{18}F]fluorouracil (**53-^{18}F**), an important PET agent in oncology, was readily obtained through aryl-Cl/^{18}F conversion followed by a simple deprotection (Fig. 4b). The key pyrimidine intermediate **52-^{18}F** obtained from easily available chloroarene **52** showed much higher labeling efficiency than previously reported aryl nickel (II) complex[30] and aryl iodonium ylide[25a]. Moreover, the precursor can be obtained in fewer synthetic steps than the diarylether analog which we previously used for radiodeoxyfluorination[29]. Taken together, our Cl/^{18}F exchange strategy offers a synthetically accessible alternative to [^{18}F]fluorouracil with high A_m[45].

We further evaluated the application of direct ^{19}F/^{18}F conversion within biologically-relevant electron rich arenes due to its exceptional efficiency and simplicity. Although the resulting PET agents may have reduced A_m, it still represents a broadly useful technology for studying the pharmacokinetics/pharmacodynamics of fluorine-containing drugs[34–36] or imaging transporter-mediated processes, such as synthesizing fluorinated amino acid agents for large neutral amino acid transporter (LAT1) imaging[46]. Amino acid metabolism represents another important class of pathways in cancer progression in addition to glucose metabolism. We were particularly interested in synthesizing ^{18}F-labeled tyrosine analogs[46]. In a proof of principle study, our direct ^{19}F/^{18}F exchange method allowed us to develop new ^{18}F-labeled tyrosine probes[47] via facile installation of ^{18}F within the aromatic core of a small library of *O*-methyl fluorotyrosine derivatives (**54–63**) (Fig. 5a). Good to excellent RCCs were observed when the fluorine nucleofuge is located at the *ortho* or *para* position relative to the methoxy group (**54**, **56**-**60**, **62**, **63**). Lower but significant labelling was

observed when the fluorine is positioned *meta* to the methoxy group (**55**, **61**). After a simple deprotection (See SI for details), ten ^{18}F-labelled *O*-methyl tyrosines were obtained and evaluated as potential PET agents in MCF7 breast cancer models. While radiotracers **54–58**, **60–62** are constitutional isomers, the relative position of ^{18}F and methoxy substitution significantly impacts their tumor uptake and clearance profiles (Fig. 5b). Most of the PET tracers demonstrated initial prominent tumor uptake at 1h post-injection followed by washout at 3h (**54-^{18}F-COOH**, **55-^{18}F-COOH**, **56-^{18}F-COOH**, **58-^{18}F-COOH, 59-^{18}F-COOH, 62-^{18}F-COOH, 63-^{18}F-COOH**). In contrast, PET agents **57-^{18}F-COOH**, **60-^{18}F-COOH, 61-^{18}F-COOH** showed high and persistent retention in the MCF-7 tumor within the same timeframe. While amino acid analogs with initial high uptake and clearance (leading to high contrast) are great candidates for imaging applications, other analogs with prolonged tumor retention provides amino acid backbones for potential therapy applications in which radioiodinated (^{131}I) or boronated (^{10}B) analogs can be used as cancer treatments via radioactive iodine therapy[48] or boron neutron capture therapy[49], respectively. Although most of the ^{18}F-labelled tyrosine analogs demonstrated apparent pancreatic uptake, introducing one extra fluorine to the arene ring (difluorinated **63-^{18}F-COOH**) greatly reduced the uptake in pancreas while still maintaining prominent tumor uptake. The effect of amino acid stereodefinition was also studied using **61-^{18}F-COOH**, which demonstrated high and persistent tumor retention. Although the contrast between the two enantiomers remained comparable at 1h post-injection (p.i.), using *L*-**61-^{18}F-COOH** doubled the tumor uptake with increased tumor retention at 3h p.i. compared with *D*-**61-^{18}F-COOH**. Taken together, these results suggest that our ^{19}F/^{18}F conversion strategy can be used to systematically investigate new PET agents with different pharmacokinetic properties for cancer imaging. Further evaluation of other *O*-methyl tyrosine enantiomers and other amino acid scaffolds are currently underway.

In addition to developing new PET agents, we are interested in applying our halide/^{18}F interconversion method to streamline the preparation of existing PET agents (Fig. 6). For example, 6-[^{18}F]Fluoro-*L*-DOPA ([^{18}F]FDOPA) is employed as an important radiopharmaceutical for Parkinson's disease (PD), brain cancer, and other diseases since the 1980s[50]. Due to its medical significance, multiple syntheses have been developed to produce [^{18}F]FDOPA for the clinical use[20a,51]. Given the readily available precursor and simply reaction procedure of our halide/^{18}F exchange approach, we evaluated our method for [^{18}F]FDOPA synthesis using *O*-methylated DOPA precursors ***L*-64-Cl** and ***L*-64-F**. We were pleased to find that radiofluorinated proceeds in 4.2% and 73.4% RCC for ***L*-64-Cl** and ***L*-64-F**, respectively. The resulting product ***L*-64-^{18}F** was easily deprotected to *L*-[^{18}F]FDOPA with 97.1% RCC and >99% enantiomeric excess (*ee*). No racemization was observed under our photoredox labeling conditions. We also found the ^{19}F/^{18}F conversion in ***L*-64-F** remains highly efficient after replacing the laser with more readily available LEDs, performing the reaction without ice cooling, reducing precursor concentration, or shortening the reaction to 5 min at room temperature. Although these conditions would lead to decreased yield, they may be more suitable for automated synthesis. The methoxymethyl (MOM)-protected analog (***L*-65**) and three constitutional isomers of DOPA (**66–68**) were efficiently labeled via Cl/^{18}F and/or direct ^{19}F/^{18}F conversion as well. Encouraged by the initial successes of our method, we explored the feasibility of synthesizing *L*-[^{18}F]FDOPA

on clinically-relevant scales. Starting from 0.93–1.11 GBq [^{18}F]TBAF, [^{18}F]FDOPA was isolated in 42% and 37.5% n.d.c. RCY (non-decay corrected radiochemical yield) when 0.01 and 0.005 mmol of ***L*-64-F** were used respectively (Fig. 6b). Further increasing the scale to ~37 GBq [^{18}F]F$^-$ leaded to > 11 GBq of [^{18}F]FDOPA with >30% n.d.c. RCY (> 99% *ee*, 1.51GBq/μmol) in 100 min (Fig. 6c). Compared with the well-established methods reported by Luxen and Lemaire[51b], our radiosynthesis has decreased A_m but features the use of a stable and readily available precursor that significantly shortens the post-radiofluorination reaction sequence. Although high A_m is not mandatory for the investigation of the neuronal dopaminergic metabolism[51a,52], we anticipate that it could be further improved by reducing precursor loading and starting from higher amounts of activity. Overall, our ^{19}F/^{18}F exchange strategy for electron-rich arenes enables a new preparation of [^{18}F]FDOPA with high enantiomeric purity from the readily available isotopic precursor. Future work will be focused on improving and automating this radiolabeling process to meet cGMP compliance standards of clinical applications.

Conclusion and Outlook

Photoredox-mediated halide/^{18}F conversion offers new inroads for the radiofluorination of electron-rich haloarenes — a limitation of current S_NAr methodology. The success of this method is most pronounced for aryl chlorides and fluorides, with the latter transformation enabling direct ^{19}F/^{18}F exchange. Its application is demonstrated by the successful radiofluorination of electron-rich halo(hetero)arenes, commercial pharmaceuticals and physiologically active compounds. Its utility for the synthesis of new PET agents is demonstrated by the rapid preparation of ^{18}F-labeled *O*-methyl tyrosine analogues and the characterization of their efficacy towards cancer imaging in breast cancer model. Lastly, direct ^{19}F/^{18}F exchange enables a scalable, late-stage radiosynthesis of [^{18}F]F-*L*-DOPA, with up to 11 GBq of the radiotracer obtained. Further improvements to this methodology, especially future work on automating this radiosynthesis protocol should enable access to new and/or clinically significant PET agents. Overall, the photoredox-mediated ^{18}F-labeling of unactivated aryl halides opens up new strategies for radiotracer synthesis via S_NAr disconnections.

Methods

General procedure for the photoredox-mediated halide/^{18}F interconversion.

Reactions were set up according to a modified literature procedure[29]. The substrate (0.01–0.05 mmol) and photocatalyst (**S1**, 1.5 mg) were weighed into a 1.5 ml eppendorf tube and transferred (with solvent when the substrate is liquid or oil) into a 5 ml V-vial via pipette. DCE (300 μl), anhydrous MeCN (45–65 μl), ^{t}BuOH(400 μl) and 25 μl of *n*-tetrabutylammonium bicarbonate ($TBAHCO_3$) in MeCN solution (~60 mg/ml) were sequentially added to the V-vial. Then a 10–30 μl aliquot of [^{18}F]TBAF in MeCN (typically 10–30 mCi) was added to the reaction vial via pipette. The reaction V-vial was then fixed either on an iron support and cooled using an ice bath or on a block without cooling. A needle connected to an N_2 filled balloon was inserted to the bottom of the V-vial and the reaction medium was continuously sparged throughout the entire reaction time. The reaction

was then irradiated top-down with a laser (MDL-D-450, 450 nm, 3.5 W after fibre coupling) (Supplementary Figure 6) or a A160WE Tuna Blue Kessil LED lamp (Supplementary Figure 7) for 30 min. The resulting solution was diluted and evenly mixed with MeCN (0.5–1ml). An aliquot of the reaction mixture (typically 300–1000 μCi) was taken for radio-HPLC analysis. The activity injected into HPLC was measured (this activity was denoted by α) and the time was recorded. The fraction corresponding to radiolabeled product was collected and the activity was measured (this activity was denoted by β) and the time was recorded. The decay-corrected β could be calculated from the recorded isolation time of each substrate. The radiochemical conversion (RCC) was obtained by dividing the decay-corrected β by α. Co-injection of the purified ^{18}F-labelled compound with commercial or synthesized ^{19}F standard via HPLC was used to confirm the identity of the radiolabeled compound.

Radio-HPLC analysis and characterization for ^{18}F-radiolabeled arenes.

All ^{18}F-labeling reactions were performed according to the general procedure unless otherwise noted. Each labeling reaction, starting activity ([^{18}F]TBAF), injected and collected activities, isolation time, decay corrected activity and calculated radiochemical conversion (RCC) are summarized in a table for each substrate. All ^{18}F-labelled products were analyzed and characterized according to the general HPLC conditions listed in supplementary information at section 3.3. Crude radio-HPLC traces of each reaction (labeled with reaction number), HPLC traces of purification and co-injection were listed. The collected ^{18}F-labeled product from crude HPLC analysis may require further HPLC-purification before co-injection with its corresponding ^{19}F standard. The red HPLC traces in the following spectra were obtained with a UV signal at 212 nm unless otherwise noted. The black HPLC traces represent the radio signal.

Synthesis of [^{18}F]FDOPA from preformed [^{18}F]TBAF.

FDOPA precursor *L*-64-F (0.01 or 0.005 mmol) and Photocatalyst S1 (1.5 mg) were dissolved in the solution of DCE/^{t}BuOH/MeCN in a 5 ml V-vial. After addition of the [^{18}F]TBAF and $TBAHCO_3$ (25 μl), the resulted solution (~1 ml) was top-down irradiated for 20 min under 450 nm laser (450 nm, 3.5 W after fibre coupling) with a N_2 balloon sparge at room temperature. The resulting reaction solution was diluted with 1 ml MeCN and passed through an aluminum cartridge (preconditioned with 5 ml DI water) to remove the unconverted ^{18}F-fluoride. Rinse the reaction vial with another 1 ml MeCN which was then passed through the same aluminum cartridge. The elution was collected in another 5 ml V-Vial and caped with a Teflon-lined septum screw cap equipped with a vent needle. The solvent was removed under 100 °C with argon stream. Argon flow was then stopped and the vent needle was removed. 200 μl HI (57 wt.% in H_2O) were then added into the V-vial and the mixture was heated under 160 °C for 10 min. A vent needle was then equipped before water (300 μl) and saturated $NaHCO_3$ solution (400 μl) was slowly added to the V-vial. The resulting aqueous solution was passed through a HPLC filter to remove the insoluble catalyst residue. The collected solution was then purified on HPLC to give the product [^{18}F]FDOPA.

Scale-up synthesis of [^{18}F]FDOPA starting from [^{18}F]F^{-}.

The aqueous solution of [^{18}F]F^{-} fluoride produced via the ^{18}O(p,n)^{18}F reaction by proton irradiation (40 μA) was delivered to a hot cell equipped with manipulators and collected in

a 5 ml V-vial containing 5 μl $TBAHCO_3$ (20%) water solution. This aqueous solution was azeotropically dried with anhydrous MeCN (1 ml × 5) under a stream of Argon at 100 °C. After removing the water, the V-vial was removed from the heater. The solution of precursor *L*-64-F (0.01 mmol) and photocatalyst (S1, 1.5 mg) in DCE/^{t}BuOH/MeCN (5/4/1, 1 ml) was then added into the V-vial. The [^{18}F]FDOPA was then obtained after the same reaction and purification procedure as the synthesis starting from preformed [^{18}F]TBAF.

Supplementary Material

Refer to Web version on PubMed Central for supplementary material.

Acknowledgments

This work was supported in part by the National Institutes of Health (NIBIB) R01EB029451 (Z.L. and D.A.N.), 5R01CA233904 (Z.L.), UNC LCCC pilot grant (Z.L. and D.A.N.), 1S10OD023611 (Z.L.) and the startup fund from UNC Department of Radiology, Biomedical Research Imaging Center, and UNC Lineberger Comprehensive Cancer Center (Z.L.)., N.E.S.T. and V.A.P are grateful for NSF Graduate Research Fellowships. We thank Dr. Gerald T. Bida for assistance with cyclotron operation, and the University of North Carolina's Department of Chemistry Mass Spectrometry Core Laboratory, especially Diane Weatherspoon, for their assistance with mass spectrometry analysis.

Data availability

All the data generated or analysed during this study are included in this article (and its Supplementary Information files).

References

1. Ametamey SM, Honer M & Schubiger PA Molecular imaging with PET. Chem. Rev 108, 1501–1516 (2008). [PubMed: 18426240]
2. Pike VW PET radiotracers: crossing the blood-brain barrier and surviving metabolism. Trends Pharmacol. Sci 30, 431–440 (2009). [PubMed: 19616318]
3. Deng XY et al. Chemistry for Positron Emission Tomography: Recent Advances in ^{11}C-, ^{18}F-, ^{13}N-, and ^{15}O-Labeling Reactions. Angew. Chem. Int. Ed 58, 2580–2605 (2019).
4. Aldeghi M, Malhotra S, Selwood DL & Chan AW Two- and three-dimensional rings in drugs. Chem. Biol. Drug Des 83, 450–461 (2014). [PubMed: 24472495]
5. Taylor RD, MacCoss M & Lawson AD Rings in drugs. J. Med. Chem 57, 5845–5859 (2014). [PubMed: 24471928]
6. Meanwell NA Fluorine and Fluorinated Motifs in the Design and Application of Bioisosteres for Drug Design. Journal of Medicinal Chemistry 61, 5822–5880 (2018). [PubMed: 29400967]
7. Zhou Y et al. Next Generation of Fluorine-Containing Pharmaceuticals, Compounds Currently in Phase II–III Clinical Trials of Major Pharmaceutical Companies: New Structural Trends and Therapeutic Areas. Chem. Rev 116, 422–518 (2016). [PubMed: 26756377]
8. Jacobson O, Kiesewetter DO & Chen XY Fluorine-18 Radiochemistry, Labeling Strategies and Synthetic Routes. Bioconjugate Chem. 26, 1–18 (2015).
9. Preshlock S, Tredwell M & Gouverneur V ^{18}F-Labeling of Arenes and Heteroarenes for Applications in Positron Emission Tomography. Chem. Rev 116, 719–766 (2016). [PubMed: 26751274]
10. van der Born D et al. Fluorine-18 labelled building blocks for PET tracer synthesis. Chem. Soc. Rev 46, 4709–4773 (2017). [PubMed: 28608906]
11. Krishnan HS, Ma LL, Vasdev N & Liang SH ^{18}F-Labeling of Sensitive Biomolecules for Positron Emission Tomography. Chem.-Eur. J 23, 15553–15577 (2017). [PubMed: 28704575]

12. Ding YS et al. Synthesis of High Specific Activity 6-[^{18}F]Fluorodopamine for Positron Emission Tomography Studies of Sympathetic Nervous-Tissue. J. Med. Chem 34, 861–863 (1991). [PubMed: 1995910]
13. Cai LS, Lu SY & Pike VW Chemistry with [^{18}F]fluoride ion. Eur. J. Org. Chem 2008, 2853–2873 (2008).
14. Quednow BB et al. Assessment of serotonin release capacity in the human brain using dexfenfluramine challenge and [^{18}F]altanserin positron emission tomography. Neuroimage 59, 3922–3932 (2012). [PubMed: 21996132]
15. Cole EL, Stewart MN, Littich R, Hoareau R & Scott PJH Radiosyntheses using Fluorine-18: The Art and Science of Late Stage Fluorination. Curr. Top. Med. Chem 14, 875–900 (2014). [PubMed: 24484425]
16. Adams DJ & Clark JH Nucleophilic routes to selectively fluorinated aromatics. Chem. Soc. Rev 28, 225–231 (1999).
17. Brooks AF, Topczewski JJ, Ichiishi N, Sanford MS & Scott PJ Late-stage [^{18}F]Fluorination: New Solutions to Old Problems. Chem. Sci 5, 4545–4553 (2014). [PubMed: 25379166]
18. Lee E et al. A Fluoride-Derived Electrophilic Late-Stage Fluorination Reagent for PET Imaging. Science 334, 639–642 (2011). [PubMed: 22053044]
19. Lee E, Hooker JM & Ritter T Nickel-Mediated Oxidative Fluorination for PET with Aqueous [^{18}F] Fluoride. J. Am. Chem. Soc 134, 17456–17458 (2012). [PubMed: 23061667]
20. (a)Tredwell M et al. A General Copper-Mediated Nucleophilic ^{18}F Fluorination of Arenes. Angew. Chem. Int. Ed 53, 7751–7755 (2014).(b)Taylor NJ et al. Derisking the Cu-Mediated 18F-Fluorination of Heterocyclic Positron Emission Tomography Radioligands. J. Am. Chem. Soc 139, 8267–8276 (2017). [PubMed: 28548849] (c)Guibbal F et al. Manual and automated Cu-mediated radiosynthesis of the PARP inhibitor [^{18}F]olaparib. Nat. Protoc 15, 1525–1541 (2020). [PubMed: 32111986]
21. (a)Chun JH, Lu SY, Lee YS & Pike VW Fast and High-Yield Microreactor Syntheses of ortho-Substituted [F-18]Fluoroarenes from Reactions of [^{18}F]Fluoride Ion with Diaryliodonium Salts. J. Org. Chem 75, 3332–3338 (2010). [PubMed: 20361793] (b)Ichiishi N et al. Copper-Catalyzed [^{18}F]Fluorination of (Mesityl)(aryl)iodonium Salts. Org. Lett 16, 3224–3227 (2014). [PubMed: 24890658]
22. Mossine AV et al. Synthesis of [^{18}F]Arenes via the Copper-Mediated [^{18}F]Fluorination of Boronic Acids. Org. Lett 17, 5780–5783 (2015). [PubMed: 26568457]
23. Makaravage KJ, Brooks AF, Mossine AV, Sanford MS & Scott PJH Copper-Mediated Radiofluorination of Arylstannanes with [^{18}F]KF. Org. Lett 18, 5440–5443 (2016). [PubMed: 27718581]
24. McCammant MS et al. Cu-Mediated C–H ^{18}F-Fluorination of Electron-Rich (Hetero)arenes. Org. Lett 19, 3939–3942 (2017). [PubMed: 28665619]
25. (a)Rotstein BH, Stephenson NA, Vasdev N & Liang SH Spirocyclic hypervalent iodine(III)-mediated radiofluorination of non-activated and hindered aromatics. Nat. Commun 5, 4365 (2014). [PubMed: 25007318] (b)Liang SH; Wang L; Stephenson NA; Rotstein BH; Vasdev N Facile ^{18}F Labeling of Non-Activated Arenes via a Spirocyclic Iodonium(III) Ylide Method and Its Application in the Synthesis of the mGluR$_5$ PET Radiopharmaceutical [^{18}F] FPEB. Nat. Protoc 14, 1530–1545 (2019). [PubMed: 30980032]
26. (a)Sander K et al. Sulfonium Salts as Leaving Groups for Aromatic Labelling of Drug-like Small Molecules with Fluorine-18. Sci. Rep 5, 9941 (2015). [PubMed: 25898175] (b)Gendron T et al. Ring-Closing Synthesis of Dibenzothiophene Sulfonium Salts and Their Use as Leaving Groups for Aromatic 18F-Fluorination. J. Am. Chem. Soc 140, 11125–11132 (2018). [PubMed: 30132661]
27. Neumann CN, Hooker JM & Ritter T Concerted nucleophilic aromatic substitution with ^{19}F$^-$ and ^{18}F$^-$. Nature 534, 369–373 (2016). [PubMed: 27281221]
28. Xu P et al. Site-Selective Late-Stage Aromatic [^{18}F]Fluorination via Aryl Sulfonium Salts. Angew. Chem. Int. Ed 59, 1956–1960 (2020).
29. Tay NES et al. ^{19}F- and ^{18}F-arene deoxyfluorination via organic photoredox-catalysed polarity-reversed nucleophilic aromatic substitution. Nat. Catal 3, 734–742 (2020). [PubMed: 33791591]

30. Hoover AJ et al. A Transmetalation Reaction Enables the Synthesis of [^{18}F]5-Fluorouracil from [^{18}F]Fluoride for Human PET Imaging. Organometallics 35, 1008–1014 (2016). [PubMed: 27087736]
31. Sharninghausen LS et al. NHC-Copper Mediated Ligand-Directed Radiofluorination of Aryl Halides. J. Am. Chem. Soc 142, 7362–7367 (2020). [PubMed: 32250612]
32. Wilcken R, Zimmermann MO, Lange A, Joerger AC & Boeckler FM Principles and Applications of Halogen Bonding in Medicinal Chemistry and Chemical Biology. J. Med. Chem 56, 1363–1388 (2013). [PubMed: 23145854]
33. Fang WY et al. Synthetic approaches and pharmaceutical applications of chloro-containing molecules for drug discovery: A critical review. Eur. J. Med. Chem 173, 117–153 (2019). [PubMed: 30995567]
34. For silicon/boron-centered ^{19}F/^{18}F exchange, see:(a)Schirrmacher R et al. ^{18}F-Labeling of Peptides by means of an Organosilicon-Based Fluoride Acceptor. Angewandte Chemie International Edition 45, 6047–6050 (2006). [PubMed: 16888726] (b)Liu Z et al. An Organotrifluoroborate for Broadly Applicable One-Step ^{18}F-Labeling. Angew. Chem. Int. Ed 53, 11876–11880 (2014).(c)Liu S et al. Lewis Acid-Assisted Isotopic ^{18}F-^{19}F Exchange in BODIPY Dyes: Facile Generation of Positron Emission Tomography/Fluorescence Dual Modality Agents for Tumor Imaging. Theranostics 3, 181–189 (2013). [PubMed: 23471211] (d)An F et al. One-Step, Rapid, ^{18}F–^{19}F Isotopic Exchange Radiolabeling of Difluoro-dioxaborinins: Substituent Effect on Stability and In Vivo Applications. J. Med. Chem 63, 12693–12706 (2020). [PubMed: 32787084]
35. For SuFEx-based strategies see:(a)Zheng Q et al. Sulfur [^{18}F]Fluoride Exchange Click Chemistry Enabled Ultrafast Late-Stage Radiosynthesis. J. Am. Chem. Soc 143, 3753–3763 (2021). [PubMed: 33630577] (b)Jeon MH et al. Late-Stage ^{18}F/^{19}F Isotopic Exchange for the Synthesis of ^{18}F-Labeled Sulfamoyl Fluorides. Org. Lett. ASAP (2021).
36. For selected examples of ^{19}F/^{18}F exchange on arenes via S_NAr for the synthesis of radiopharmaceuticals, see:(a)Langer O et al. Synthesis of fluorine-18-labeled Ciprofloxacin for PET studies in humans. Nucl. Med. Biol 30, 285–291 (2003). [PubMed: 12745020] (b)Rokka J et al. ^{19}F/^{18}F exchange synthesis for a novel [^{18}F]S1P$_3$-radiopharmaceutical. J. Label. Compd. Radiopharm 56, 385–391 (2013).
37. Chen W et al. Direct arene C–H fluorination with $^{18}F^-$ via organic photoredox catalysis. Science 364, 1170–1174 (2019). [PubMed: 31221856]
38. Zweig Arnold., Hodgson, W. G. & Jura, W. H. The Oxidation of Methoxybenzenes. J. Am. Chem. Soc 86, 4124–4129 (1964).
39. (a)Blom E, Karimi F & Langstrom B [^{18}F]/^{19}F exchange in fluorine containing compounds for potential use in ^{18}F -labelling strategies. J. Label. Compd. Radiopharm 52, 504–511 (2009). (b)Wagner FM, Ermert J & Coenen HH Three-Step, “One-Pot” Radiosynthesis of 6-Fluoro-3,4-Dihydroxy-*L*-Phenylalanine by Isotopic Exchange. J. Nucl. Med 50, 1724–1729 (2009). [PubMed: 19759110] (c)Weiss PS, Ermert J, Melean JC, Schafer D & Coenen HH Radiosynthesis of 4-[^{18}F]fluoro-*L*-tryptophan by isotopic exchange on carbonyl-activated precursors. Bioorg. Med. Chem 23, 5856–5869 (2015). [PubMed: 26193761]
40. Liu Z et al. An organotrifluoroborate for broadly applicable one-step ^{18}F-labeling. Angew. Chem. Int. Ed 53, 11876–11880 (2014).
41. (a)Tay NES & Nicewicz DA Cation Radical Accelerated Nucleophilic Aromatic Substitution via Organic Photoredox Catalysis. J. Am. Chem. Soc 139, 16100–16104 (2017). [PubMed: 29068677] (b)Holmberg-Douglas N & Nicewicz DA Arene Cyanation via Cation-Radical Accelerated-Nucleophilic Aromatic Substitution. Org. Lett 21, 7114–7118, (2019). [PubMed: 31418275] (c)Venditto NJ & Nicewicz DA Cation Radical-Accelerated Nucleophilic Aromatic Substitution for Amination of Alkoxyarenes. Org. Lett 22, 4817–4822, (2020). [PubMed: 32484681]
42. Shewchuk L et al. Binding mode of the 4-anilinoquinazoline class of protein kinase inhibitor: X-ray crystallographic studies of 4-anilinoquinazolines bound to cyclin-dependent kinase 2 and p38 kinase. J. Med. Chem 43, 133–138, (2000). [PubMed: 10633045]
43. Olberg DE et al. Synthesis and *in vitro* evaluation of small-molecule [^{18}F] labeled gonadotropin-releasing hormone (GnRH) receptor antagonists as potential PET imaging agents for GnRH receptor expression. Bioorg. Med. Chem. Lett 24, 1846–1850 (2014). [PubMed: 24613701]

44. (a)Vivash L & O'Brien TJ Imaging Microglial Activation with TSPO PET: Lighting Up Neurologic Diseases? J. Nucl. Med 57, 165–168 (2016). [PubMed: 26697963] (b)Alam MM, Lee J & Lee SY Recent Progress in the Development of TSPO PET Ligands for Neuroinflammation Imaging in Neurological Diseases. Nucl. Med Mol. Imaging 51, 283–296 (2017). [PubMed: 29242722] (c)Werry EL et al. Recent Developments in TSPO PET Imaging as A Biomarker of Neuroinflammation in Neurodegenerative Disorders. Int. J. Mol. Sci 20, 3161 (2019).

45. Historical syntheses of [^{18}F]fluorouracil involve direct fluorination of uracil with [^{18}F]F_2; seeOberdorfer F, Hofmann E & Maierborst W Preparation of F-18-Labeled 5-Fluorouracil of Very High-Purity. J. Label. Compd. Radiopharm 27, 137–145 (1989).

46. (a)Fuchs BC & Bode BP Amino acid transporters ASCT2 and LAT1 in cancer: Partners in crime? Seminars in Cancer Biology 15, 254–266 (2005). [PubMed: 15916903] (b)Wang Q & Holst J *L*-type amino acid transport and cancer: targeting the mTORC1 pathway to inhibit neoplasia. Am. J. Cancer Res 5, 1281–1294 (2015). [PubMed: 26101697] (c)Qi YQ, Liu XH, Li J, Yao HQ & Yuan SH Fluorine-18 labeled amino acids for tumor PET/CT imaging. Oncotarget 8, 60581–60588 (2017). [PubMed: 28947996] (d)Sun AX, Liu X & Tang GH Carbon-11 and Fluorine-18 Labeled Amino Acid Tracers for Positron Emission Tomography Imaging of Tumors. Front. Chem 5, 124 (2018). [PubMed: 29379780]

47. (a)Langen KJ et al. *O*-(2-[^{18}F]fluoroethyl)-L-tyrosine: uptake mechanisms and clinical applications. Nucl. Med. Biol 33, 287–294 (2006). [PubMed: 16631076] (b)Zoghbi SS et al. PET imaging of the dopamine transporter with ^{18}F-FECNT: A polar radiometabolite confounds brain radioligand measurements. J. Nucl. Med 47, 520–527 (2006). [PubMed: 16513622] (c)Franck D et al. Investigations into the synthesis, radiofluorination and conjugation of a new [^{18}F]fluorocyclobutyl prosthetic group and its *in vitro* stability using a tyrosine model system. Bioorg. Med. Chem 21, 643–652 (2013). [PubMed: 23290251] (d)Kuchar M & Mamat C Methods to Increase the Metabolic Stability of ^{18}F-Radiotracers. Molecules 20, 16186–16220 (2015). [PubMed: 26404227] (e)Stegmayr C, Willuweit A, Lohmann P & Langen KJ *O*-(2-[^{18}F]-Fluoroethyl)-*L*-Tyrosine (FET) in Neurooncology: A Review of Experimental Results. Curr. Radiopharm 12, 201–210 (2019). [PubMed: 30636621]

48. Lee SL Radioactive iodine therapy. Curr. Opin. Endocrinol. Diabetes Obes 19, 420–428 (2012). [PubMed: 22914564]

49. Barth RF, Mi P & Yang W Boron delivery agents for neutron capture therapy of cancer. Cancer Comm. 38, 35 (2018).

50. Garnett ES, Firnau G & Nahmias C Dopamine Visualized in the Basal Ganglia of Living Man. Nature 305, 137–138 (1983). [PubMed: 6604227]

51. For a minireview, see:(a)Pretze M, Wängler C & Wängler B 6-[^{18}F]Fluoro-L-DOPA: A Well-Established Neurotracer with Expanding Application Spectrum and Strongly Improved Radiosyntheses. BioMed Research International 2014, e674063 (2014).For specific methods, see: (b)Libert LC et al. Production at the Curie Level of No-Carrier-Added 6-^{18}F-Fluoro-*L*-Dopa. J. Nucl. Med 54, 1154–1161 (2013). [PubMed: 23658219] (c)Lemaire C et al. Automated production at the curie level of no-carrier-added 6-[^{18}F]fluoro-*L*-dopa and 2-[^{18}F]fluoro-*L*-tyrosine on a FASTlab synthesizer. J. Label. Compd. Radiopharm 58, 281–290 (2015).(d)Preshlock S et al. Enhanced copper-mediated ^{18}F-fluorination of aryl boronic esters provides eight radiotracers for PET applications. Chem. Commun 52, 8361–8364 (2016).(e)Luurtsema G et al. Improved GMP-compliant multi-dose production and quality control of 6-[^{18}F]fluoro-*L*-DOPA. EJNMMI Radiopharm. Chem 1, 7 (2017). [PubMed: 29564384] (f)Zarrad F, Zlatopolskiy BD, Krapf P, Zischler J & Neumaier B A Practical Method for the Preparation of ^{18}F-Labeled Aromatic Amino Acids from Nucleophilic [^{18}F]Fluoride and Stannyl Precursors for Electrophilic Radiohalogenation. Molecules 22, 2231 (2017).(g)Mossine AV et al. One-pot synthesis of high molar activity 6-[^{18}F]fluoro-*L*-DOPA by Cu-mediated fluorination of a BPin precursor. Org. Biomol. Chem 17, 8701–8705, (2019). [PubMed: 31536095] (h)Mossine AV et al. Synthesis of high-molar-activity [^{18}F]6-fluoro-*L*-DOPA suitable for human use via Cu-mediated fluorination of a BPin precursor. Nature Protocols 15, 1742–1759 (2020). [PubMed: 32269382] (i)Orlovskaya V, Fedorova O, Kuznetsova O & Krasikova R Cu-Mediated Radiofluorination of Aryl Pinacolboronate Esters: Alcohols as Solvents with Application to 6-*L*-[^{18}F]FDOPA Synthesis. Eur. J. Org. Chem 2020, 7079–7086 (2020).For a review on Cu-mediated radiofluorination of arylboronates and arylstannanes for the synthesis of [^{18}F]FDOPA, see(j)Krasikova RN

Nucleophilic Synthesis of 6-*L*-[^{18}F]FDOPA. Is Copper-Mediated Radiofluorination the Answer? Molecules 25, 4365 (2020).

52. Luxen A et al. Production of 6-[^{18}F]Fluoro-*L*-Dopa and its metabolism *in vivo* - a critical-review. Int. J. Rad. Appl. Instrum. B 19, 149–158 (1992). [PubMed: 1601668]

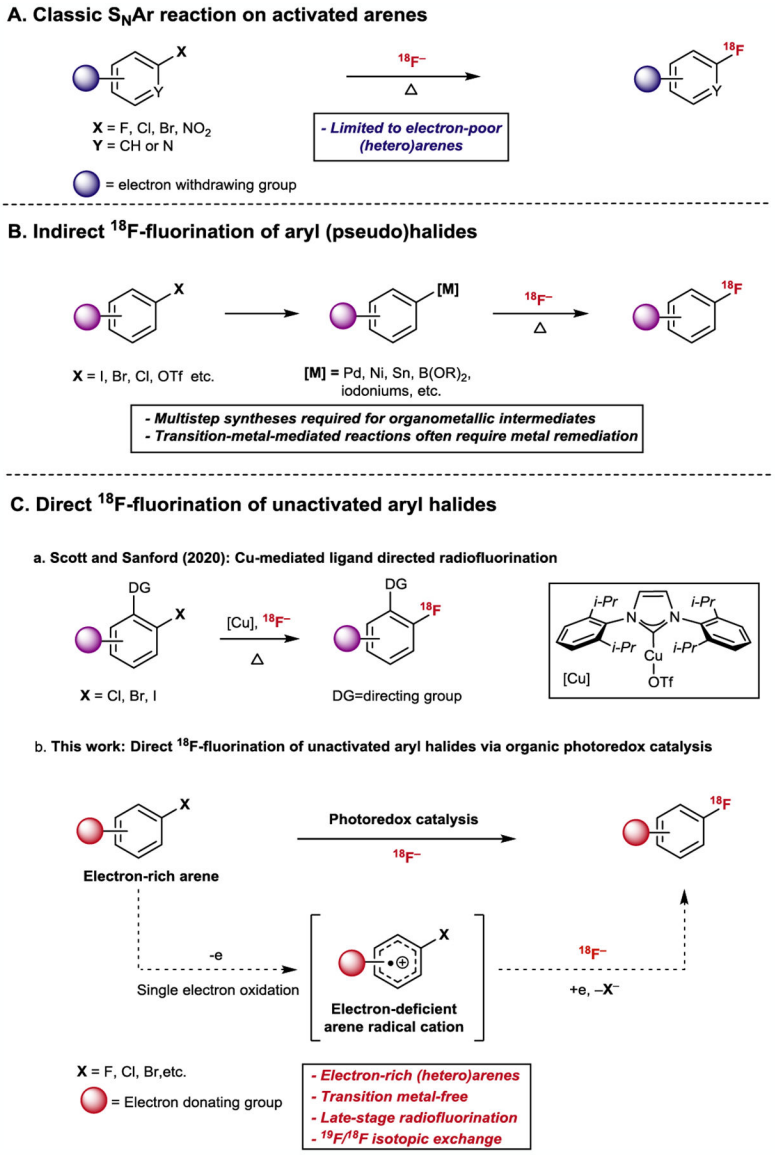

Fig.1 |. Nucleophilic arene ^{18}F-fluorination.

(A) S_NAr reaction on activated (electron-deficent) arenes (B) Indirect ^{18}F-fluorination of aryl(pseudo) halides (C) Direct ^{18}F-fluorination of aryl halides

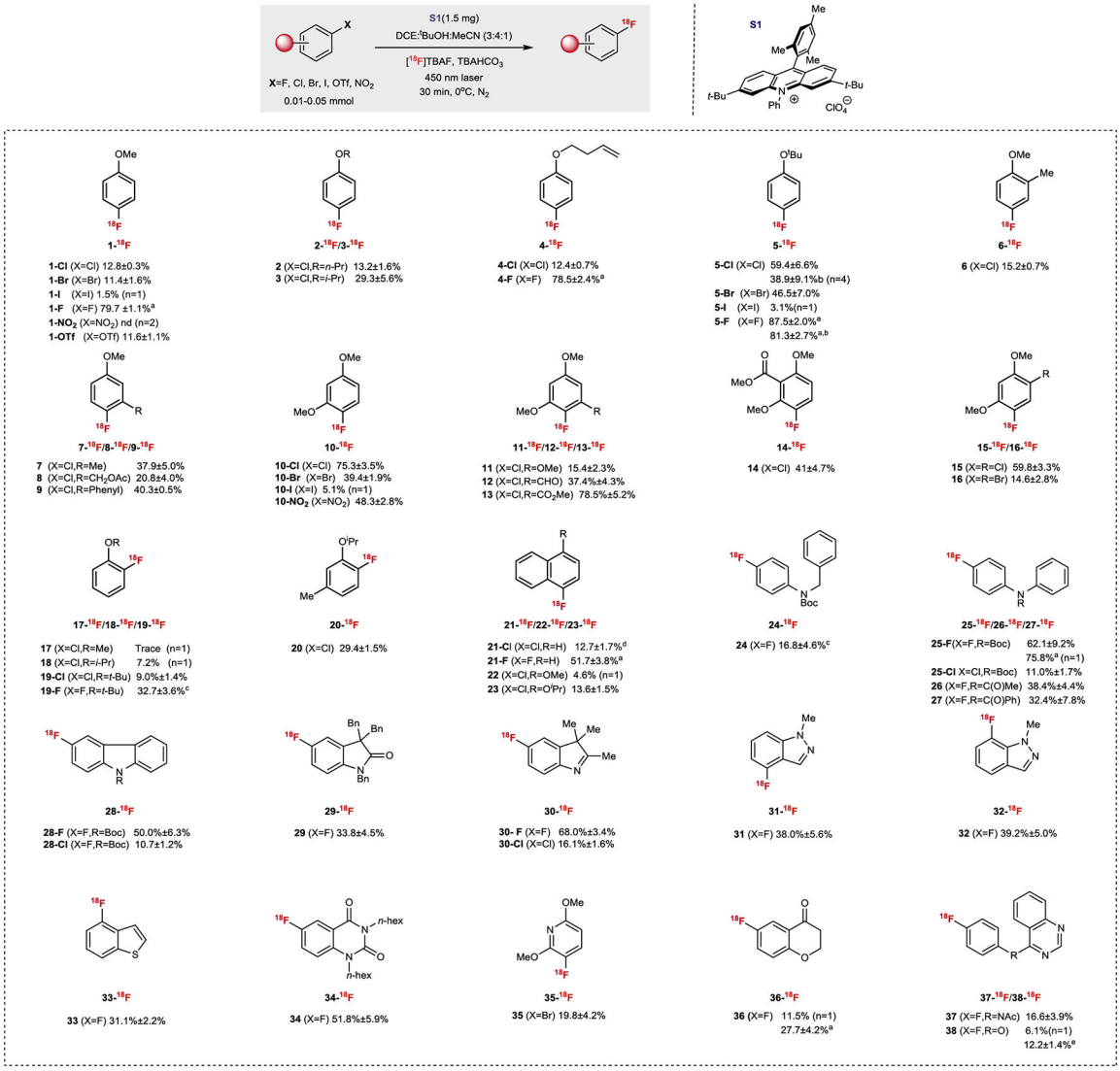

Fig.2 |. Reaction scope of direct ^{18}F-fluorination of aryl halides via halide/^{18}F interconversion. All radiochemical conversions (RCCs) were calculated by HPLC isolation and averaged over 3 experiments unless otherwise noted. 0.37–1.11 GBq [^{18}F]TBAF were generally used for the labeling. 0.05 mmol substrate were used for all the labeling reactions except Ar-F which used 0.01 mmol unless otherwise noted. [a]0.05 mmol substrate. [b]Blue LED instead of laser. [c]0.02 mmol substrate. [d]0.1 mmol substrate. [e]Reaction was performed under air.

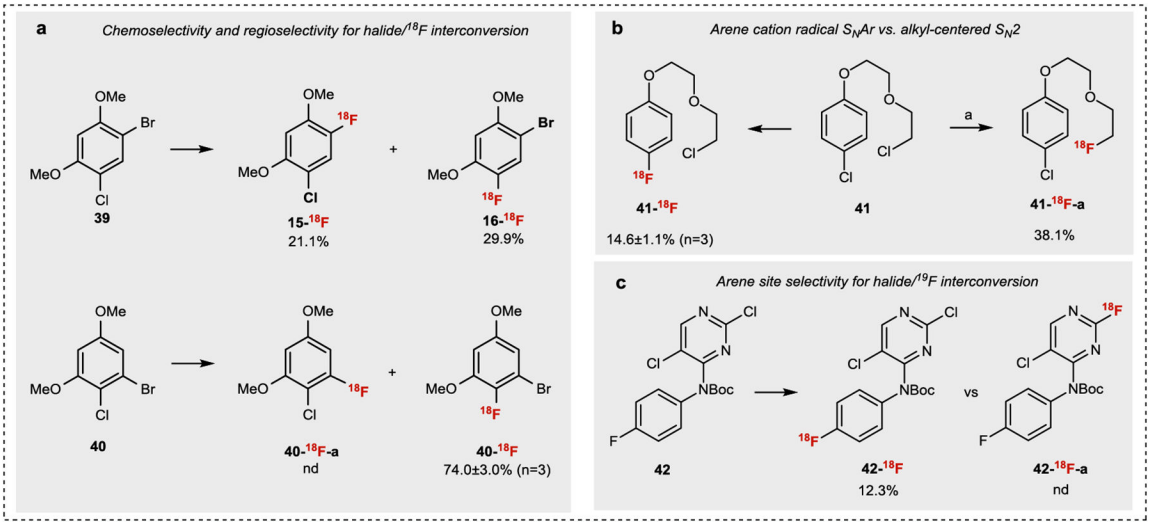

Fig.3 |. Chemo-and regioselectivity study of aryl halide/^{18}F interconversion.

All halide/^{18}F interconversion reactions were conducted under standard conditions listed in Fig.2. **a**. Comparison of reactivity between ArBr and ArCl. **b**. Comparison of reactivity between SNAr and SN2 under light condition. **c.** Comparison of reactivity between electron rich and electron deficient aromatic rings. [a][^{18}F]TBAF, MeCN, 100°C, 10 min (See SI for details).

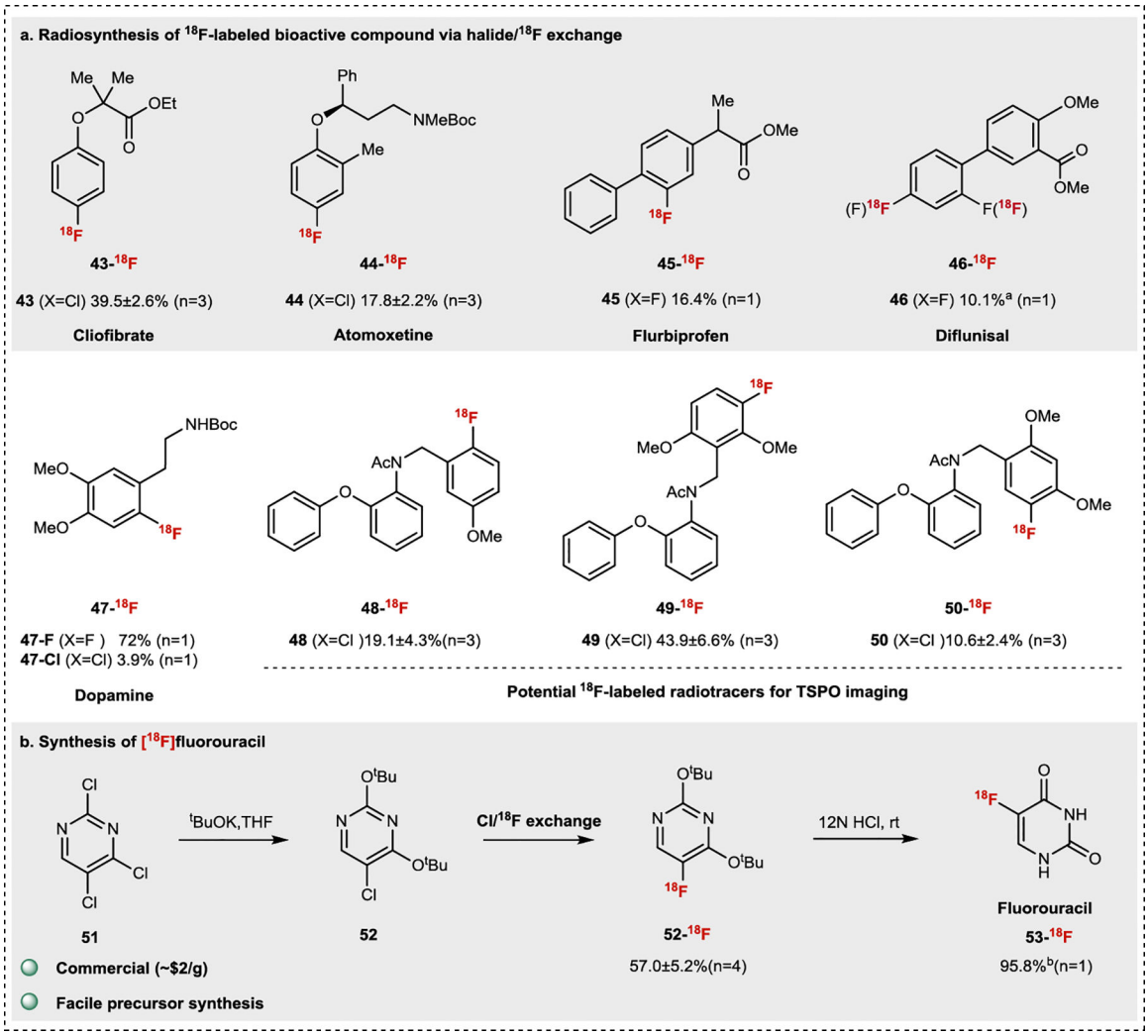

Fig.4 |. Application of the halide/^{18}F interconversion to late-stage radiofluorination.

All halide/^{18}F exchange reactions were conducted under standard conditions listed in Fig.2. **a**. Labeling of bioactive compounds. **b**. Synthesis of [^{18}F]fluorouracil. [a]0.05 mmol substrate. [b]Deprotection yield.

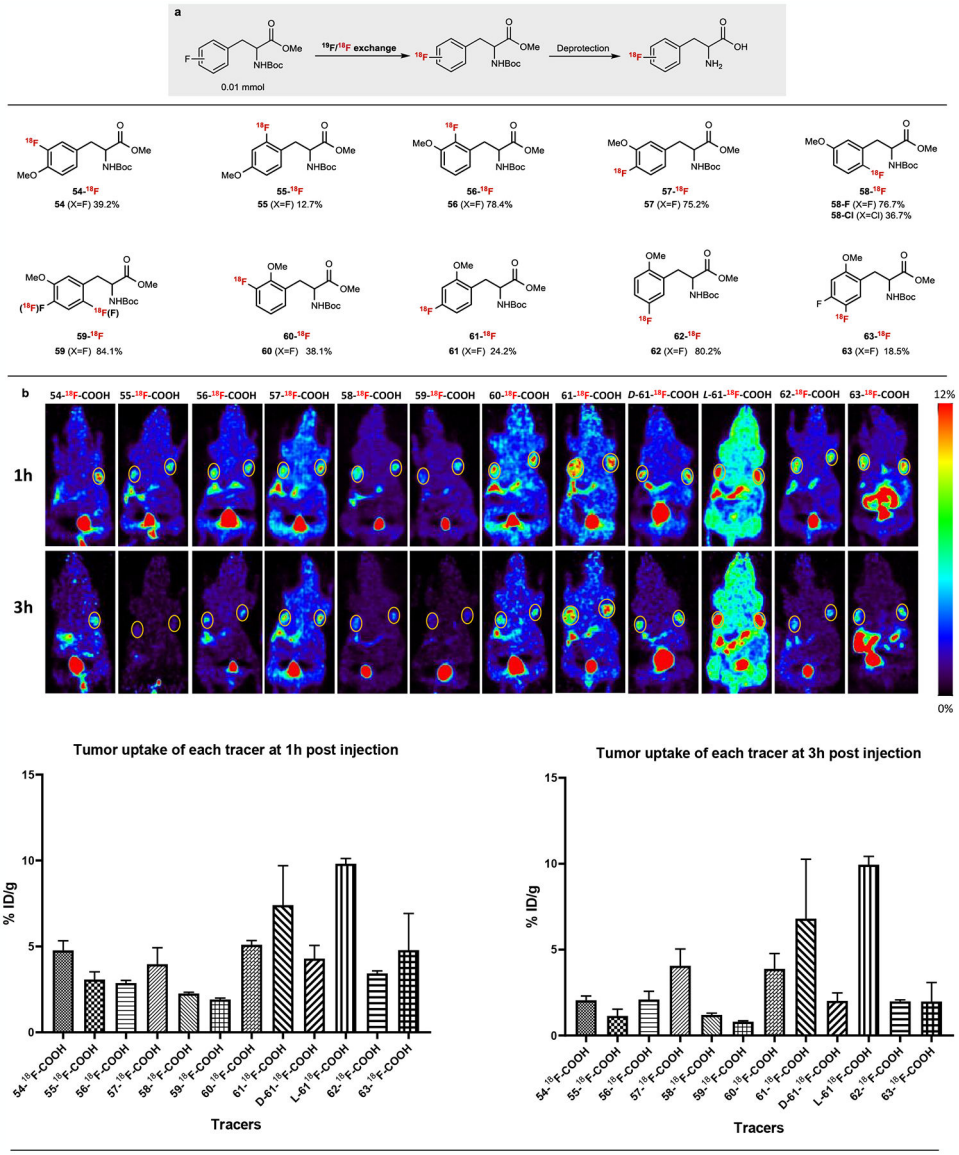

Fig.5 |. Screening of ^{18}F-labeled *O*-methyl tyrosines in a MCF7 (breast cancer) tumor model system.

All halide/^{18}F exchange reactions were conducted under standard conditions listed in Fig 2. **a.** Radiosynthesis of ^{18}F-labeled tyrosines, **b.** PET imaging of ^{8}F-labeled tyrosines in the MCF7 tumor model system (circled in the pictures)

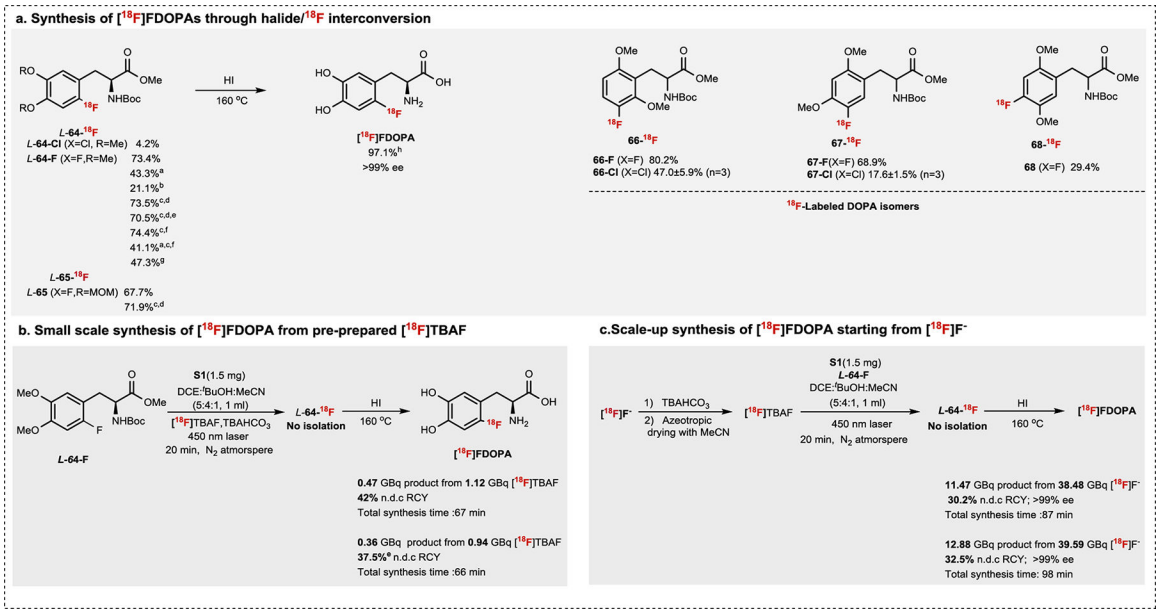

Fig.6 |. Synthesis of [^{18}F]FDOPA.

All halide/^{18}F interconversion reactions were conducted under standard condition listed on Fig.2 unless otherwise noted. Radiochemical conversions (RCCs) were calculated by HPLC isolation. 0.05 mmol substrates were used for Cl/^{18}F exchange labeling reactions; 0.01 mmol substrate used for ^{19}F/^{18}F exchange reaction unless otherwise noted. [a]Blue LED was used instead of laser. [b]No DCE were added in the reaction. [c]No ice cooling and 500 μl DCE were used. [d]Reaction ran 20 min. [e]0.005 mmol substrate. [f]Reaction ran 5 min. [g]air bubbling instead of N_2. [h]Deprotection yield.